OAK RIDGE NATIONAL LABORATORY
operated by
UNION CARBIDE CORPORATION • NUCLEAR DIVISION
for the
U.S. ATOMIC ENERGY COMMISSION

ORNL-TM- 3739

DATE - April 3, 1972

Neutron Physics Division

# MONTE CARLO CALCULATIONS OF THE RESPONSE FUNCTIONS OF BONNER BALL NEUTRON DETECTORS

C. E. Burgart† and M. B. Emmett*

## Abstract

Adjoint MORSE calculations were performed to verify the response functions of Bonner ball neutron detectors. Bare 3-in.- and 6-in.-diameter Bonner balls were considered. These calculations utilized 123-group cross sections with 30 groups of thermal upscatter and also 104-group cross sections with a single thermal group. The response function shapes are in good agreement and the magnitudes are within 10% of previously reported results.

†Present Address: Science Applications, Inc., Albuquerque, N. M. 87108

*Mathematics Division.

BLANK PAGE

Adjoint MORSE Monte Carlo calculations[1-3] were performed to verify the response functions of several Bonner ball neutron detectors. These calculations utilized 123-group cross sections ($P_3$) with 30 thermal groups of upscatter and also 104-group cross sections ($P_3$) with a single thermal group. The 123-group cross sections were generated via the XLACS route,[4] and the 104-group cross sections via SUPERTOG.[5] The basic neutron cross sections were from ENDF/B-II data. The results of these calculations are compared with previous results[6,7] obtained with ANISN.

The energy spectrum of the source in the adjoint Monte Carlo calculations was the macroscopic (n,$\alpha$) cross section for $^{10}B$ at a density of 1.275 x $10^{-5}$ atoms/barn·cm. The spatial and angular distributions were uniform and isotropic in a sphere of radius 2.54 cm. This active volume is 5.6% larger than that in the previous calculations. However, the previous calculations (at least the bare case) were performed for a 4% higher density (1.328 x $10^{-5}$ atoms/barn·cm). These differences tend to offset each other.

The configuration consisted of a sphere of $^{10}B$ of radius 2.54 cm and density 1.275 x $10^{-5}$ atoms/barn·cm surrounded by a spherical shell of polyethylene of density 0.951 grams/cc. Two polyethylene thicknesses were investigated, 1.1938 and 5.00 cm. The $^{11}B$, fluorine, copper shell and cadmium cover were not included. The energy-dependent current leaking from the configuration was calculated. This corresponds to the response function for an isotropic source incident on the detector.

The non-absorption weighting in adjoint Monte Carlo calculations can cause large weight fluctuations, and hence, poor statistics. To mitigate this problem, Russian roulette and splitting were utilized to maintain the particle weights within a factor of 10 of the starting weight. The results of these calculations are presented as counts/incident neutron/cm$^2$, where the MORSE results have been multiplied by the detector

BLANK PAGE

efficiencies given in reference 7.

Table 1 and Fig. 1 contain the responses above 1.855 eV for the bare $BF_3$ detector. Table 1 gives the results for both the 123-group and 104-group calculations. The estimated fractional standard deviations of the Monte Carlo results are given in parentheses. Figure 1 indicates that the Monte Carlo 123-group results are consistently high (5-10%) when compared with the ANISN calculation; however, the shape is in quite good agreement. Though not plotted, the 104-group Monte Carlo results are very close to the ANISN calculations, both in shape and magnitude.

Table 2 and Figs. 2-4 present responses for the 3-in. and 6-in. Bonner balls. The two Monte Carlo calculations and the ANISN calculation are in excellent agreement for the 3-in. Bonner ball. The 123-group Monte Carlo results for the 6-in. case appear to be higher than the previous ANISN results; however, the shapes are in good agreement. (The results in Fig. 4,indicated as 123-group new results, are discussed in the Addendum.) The approximate average difference in magnitude is less than 10%. This difference may be within the limits of accuracy of the techniques. The results of a 104-group calculation for the 6-in. Bonner ball are not shown due to statistical difficulties that were caused by "strange but true" non-absorption weighting.

In order to investigate the effect of the response due to $^{10}B(n,\alpha)$ reactions above a few eV, a MORSE case was run in which the adjoint source was zeroed above 1.855 eV. The resulting response function for the 6-in. Bonner ball is compared with the MORSE results with the full source in Fig. 5. The magnitude was reduced 10-20%; however, the shape was affected very little. This indicates that independent of incident energy, 80% or more of the incident neutrons are detected after they slow down to below

Table 1. Bare $BF_3$ Response Functions

| Top Edge of Energy Group (eV) | 123-Group Results × 0.525 (counts/incident neutron/cm$^2$) | 104-Group Results × 0.525 (counts/incident neutron/cm$^2$) |
|---|---|---|
| 1.855 | | |
| 2.382 | 0.201(0.011) | 0.185(0.018) |
| 3.059 | 0.175(0.014) | 0.167(0.021) |
| 3.928 | 0.157(0.015) | 0.146(0.020) |
| 5.043 | 0.139(0.017) | 0.130(0.023) |
| 6.476 | 0.125(0.017) | 0.119(0.022) |
| 8.315 | 0.107(0.018) | 0.098(0.027) |
| 1.068(+1)[a] | 0.095(0.017) | 0.092(0.025) |
| 1.371 | 0.083(0.020) | 0.077(0.031) |
| 1.760 | 0.076(0.022) | 0.072(0.032) |
| 2.260 | 0.066(0.021) | 0.061(0.033) |
| 2.902 | 0.0578(0.026) | 0.0523(0.034) |
| 3.727 | 0.0525(0.024) | 0.0493(0.036) |
| 4.785 | 0.0438(0.024) | 0.0428(0.037) |
| 6.144 | 0.0390(0.029) | 0.0370(0.041) |
| 7.889(+1) | 0.0355(0.033) | 0.0347(0.038) |
| 1.013(+2) | 0.0298(0.030) | 0.0275(0.048) |
| 1.301 | 0.0271(0.038) | 0.0267(0.054) |
| 1.670 | 0.0249(0.039) | 0.0252(0.048) |
| 2.144 | 0.0229(0.040) | 0.0210(0.058) |
| 2.754 | 0.0187(0.046) | 0.0185(0.061) |
| 3.536 | 0.0149(0.045) | 0.0145(0.078) |
| 4.540 | 0.0144(0.046) | 0.0143(0.074) |
| 5.829 | 0.0132(0.048) | 0.0126(0.072) |
| 7.485 | 0.0116(0.045) | 0.0101(0.082) |
| 9.611(+2) | 0.0100(0.065) | 0.0092(0.094) |
| 1.234(+3) | 0.0076(0.071) | 0.0078(0.088) |
| 1.585 | 0.0069(0.071) | 0.0068(0.088) |
| 2.035 | 0.0068(0.068) | 0.0058(0.095) |
| 2.613 | 0.0063(0.076) | 0.0056(0.099) |
| 3.355 | 0.0057(0.078) | 0.0063(0.098) |
| 4.307 | 0.0051(0.081) | 0.0055(0.106) |
| 5.531 | 0.0041(0.083) | 0.0042(0.123) |
| 7.102 | 0.0036(0.090) | 0.0039(0.143) |
| 9.119(+3) | 0.0034(0.092) | 0.0034(0.139) |
| 1.171(+4) | 0.0030(0.097) | 0.0030(0.134) |
| 1.503(+4) | 0.0025(0.115) | 0.0031(0.135) |

[a] Read as 1.068 x $10^1$.

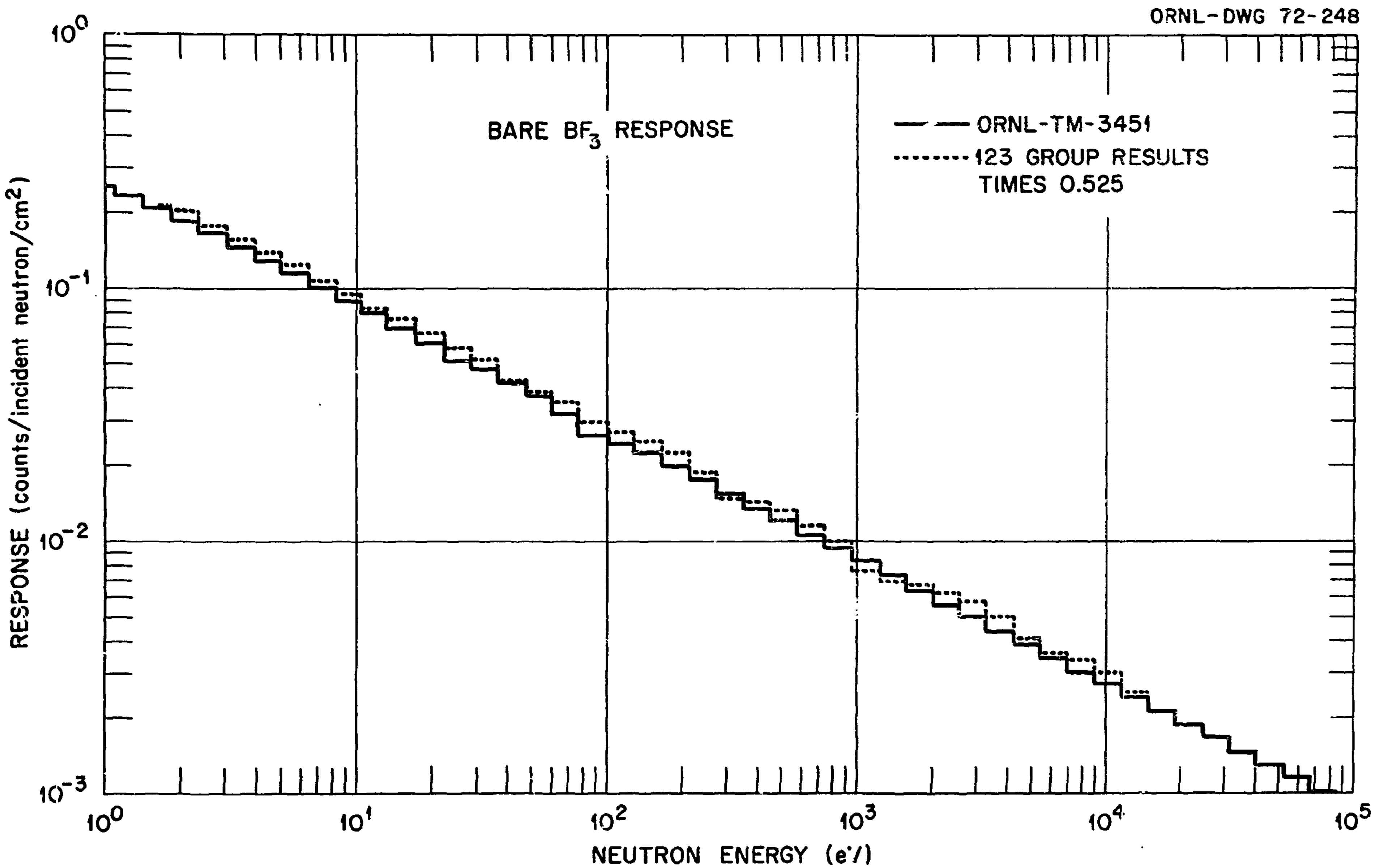


Fig. 1. Comparison Between ANISN and MORSE Calculated Bare $BF_3$ Counter Response Functions.

Table 2, Bonner Ball Response Functions

| | 3-in.-Diameter Bonner Ball (0.47 in. Poly.) | | 6-in.-Diam. BB (1.97 in. Poly.) |
|---|---|---|---|
| Top Edge of Energy Group (eV) | MORSE 123-Group Results × 0.470 | MORSE 104-Group Results × 0.470 | MORSE 123-Group Calc. × 0.443 |
| | (counts/incident neutron/cm$^2$) | | |
| 1.855 | | | |
| 2.382 | 1.39(0.041)[b] | 1.52(0.069) | |
| 3.059 | 1.45(0.033) | 1.51(0.071) | |
| 3.428 | 1.33(0.040) | 1.48(0.068) | |
| 5.043 | 1.27(0.043) | 1.41(0.067) | |
| 6.476 | 1.23(0.043) | 1.41(0.067) | |
| 8.315 | 1.24(0.039) | 1.33(0.063) | |
| 1.068(+1)[a] | 1.21(0.036) | 1.31(0.065) | |
| 1.371 | 1.17(0.035) | 1.24(0.063) | |
| 1.760 | 1.16(0.039) | 1.21(0.067) | |
| 2.260 | 1.14(0.048) | 1.17(0.065) | |
| 2.902 | 1.09(0.042) | 1.12(0.063) | |
| 3.727 | 0.99(0.044) | 1.07(0.066) | |
| 4.785 | 0.93(0.050) | 1.02(0.069) | |
| 6.144 | 0.94(0.047) | 0.99(0.060) | |
| 7.889(+1) | 0.97(0.047) | 0.94(0.068) | |
| 1.013(+2) | 0.87(0.055) | 0.91(0.065) | 1.12(0.111) |
| 1.301 | 0.81(0.046) | 0.90(0.065) | 1.04(0.107) |
| 1.670 | 0.77(0.054) | 0.86(0.064) | 1.16(0.108) |
| 2.144 | 0.75(0.049) | 0.80(0.064) | 1.02(0.119) |
| 2.754 | 0.70(0.056) | 0.75(0.066) | 1.00(0.067) |
| 3.536 | 0.62(0.054) | 0.73(0.062) | 1.14(0.092) |
| 4.540 | 0.68(0.049) | 0.69(0.066) | 1.17(0.052) |
| 5.830 | 0.61(0.054) | 0.67(0.066) | 1.16(0.057) |
| 7.485 | 0.61(0.060) | 0.64(0.070) | 1.10(0.116) |
| 9.611(+2) | 0.570(0.054) | 0.62(0.068) | 1.16(0.097) |
| 1.234(+3) | 0.555(0.059) | 0.556(0.066) | 1.24(0.096) |
| 1.585 | 0.461(0.058) | 0.549(0.070) | 1.28(0.089) |
| 2.035 | 0.478(0.052) | 0.514(0.072) | 1.15(0.129) |
| 2.613 | 0.444(0.060) | 0.524(0.067) | 1.10(0.073) |
| 3.355 | 0.393(0.065) | 0.478(0.067) | 1.18(0.092) |
| 4.307 | 0.388(0.066) | 0.458(0.068) | 1.27(0.103) |
| 5.531 | 0.392(0.058) | 0.433(0.068) | 1.27(0.083) |
| 7.102 | 0.387(0.068) | 0.430(0.069) | 1.25(0.054) |
| 9.119(+3) | 0.369(0.063) | 0.399(0.071) | 1.20(0.096) |

Table 2 (continued)

| | 3-in.-Diameter Bonner Ball (0.47 in. Poly.) | | 6-in.-Diam. BB (1.97 in. Poly.) |
|---|---|---|---|
| Top Edge of Energy Group (eV) | MORSE 123-Group Results × 0.470 | MORSE 104-Group Results × 0.470 | MORSE 123-Group Calc. × 0.443 |
| | (counts/incident neutron/cm$^2$) | | |
| 1.171(+4) | 0.384(0.059) | 0.378(0.066) | 1.22(0.087) |
| 1.503 | 0.359(0.069) | 0.357(0.070) | 1.17(0.071) |
| 1.931 | 0.306(0.073) | 0.350(0.065) | 1.19(0.076) |
| 2.479 | 0.302(0.060) | 0.316(0.069) | 1.25(0.095) |
| 3.183 | 0.307(0.067) | 0.311(0.068) | 1.28(0.071) |
| 4.087 | 0.258(0.073) | 0.278(0.068) | 1.31(0.063) |
| 5.248 | 0.257(0.071) | 0.273(0.066) | 1.33(0.077) |
| 6.738 | 0.224(0.091) | 0.246(0.077) | 1.35(0.072) |
| 8.612(+4) | 0.220(0.088) | 0.250(0.066) | 1.36(0.075) |
| 1.111(+5) | 0.197(0.070) | 0.228(0.075) | 1.28(0.060) |
| 1.228 | 0.168(0.091) | 0.201(0.073) | 1.57(0.070) |
| 1.357 | 0.183(0.116) | 0.191(0.073) | 1.54(0.101) |
| 1.500 | 0.203(0.083) | 0.186(0.076) | 1.41(0.058) |
| 1.657 | 0.173(0.099) | 0.181(0.080) | 1.45(0.073) |
| 1.832 | 0.156(0.094) | 0.181(0.067) | 1.55(0.073) |
| 2.024 | 0.141(0.108) | 0.145(0.074) | 1.41(0.061) |
| 2.237 | 0.117(0.088) | 0.158(0.080) | 1.50(0.088) |
| 2.472 | 0.131(0.102) | 0.142(0.074) | 1.50(0.075) |
| 2.732 | 0.131(0.085) | 0.143(0.071) | 1.62(0.052) |
| 3.020 | 0.130(0.091) | 0.122(0.078) | 1.46(0.068) |
| 3.337 | 0.112(0.093) | 0.136(0.075) | 1.54(0.055) |
| 3.688 | 0.109(0.094) | 0.117(0.083) | 1.59(0.069) |
| 4.076 | 0.131(0.088) | 0.113(0.081) | 1.52(0.075) |
| 4.505 | 0.105(0.105) | 0.115(0.076) | 1.58(0.055) |
| 4.979 | 0.102(0.102) | 0.101(0.075) | 1.64(0.080) |
| 5.502 | 0.081(0.134) | 0.090 (0.072) | 1.56(0.065) |
| 6.081 | 0.093(0.121) | 0.089 (0.075) | 1.48(0.061) |
| 6.721 | 0.067(0.108) | 0.076 (0.095) | 1.73(0.043) |
| 7.427 | 0.075(0.118) | 0.073 (0.084) | 1.55(0.077) |
| 8.209 | 0.063(0.136) | 0.063 (0.088) | 1.54(0.062) |
| 9.072(+5) | 0.071(0.128) | 0.065 (0.100) | 1.64(0.060) |
| 1.003(+6) | 0.056(0.125) | 0.0542(0.086) | 1.53(0.074) |
| 1.108 | | 0.0565(0.092) | 1.42(0.067) |
| 1.225 | | 0.0500(0.085) | 1.51(0.083) |
| 1.353(+6) | | 0.0464(0.097) | 1.29(0.049) |

Table 2 (continued)

| | 3-in.-Diameter Bonner Ball (0.47 in. Poly.) | | 6-in.-Diam. BB (1.97 in. Poly.) |
|---|---|---|---|
| Top Edge of Energy Group (eV) | MORSE 123-Group Results × 0.470 | MORSE 104-Group Results × 0.470 | MORSE 123-Group Calc. × 0.443 |
| | (counts/incident neutron/cm²) | | |
| 1.496(+6) | | 0.0416(0.100) | 1.33(0.060) |
| 1.653 | | 0.0405(0.096) | 1.25(0.065) |
| 1.827 | | 0.0338(0.086) | 1.30(0.076) |
| 2.020 | | 0.0346(0.097) | 1.24(0.066) |
| 2.231 | | 0.0277(0.102) | 1.22(0.065) |
| 2.466 | | 0.0234(0.118) | 1.09(0.064) |
| 2.725 | | 0.0216(0.123) | 1.09(0.065) |
| 3.012 | | 0.0188(0.119) | 0.92(0.065) |
| 3.329 | | 0.0187(0.110) | 0.94(0.091) |
| 3.679 | | | 0.81(0.074) |
| 4.066 | | | 0.77(0.082) |
| 4.493 | | | 0.82(0.086) |
| 4.966 | | | 0.69(0.077) |
| 5.488 | | | 0.61(0.068) |
| 6.065 | | | 0.67(0.072) |
| 6.703 | | | 0.566(0.093) |
| 7.408 | | | 0.511(0.078) |
| 8.187 | | | 0.465(0.086) |
| 9.048(+6) | | | 0.390(0.065) |
| 1.000(+7) | | | 0.376(0.094 |
| 1.105 | | | 0.288(0.094) |
| 1.221 | | | 0.294(0.069) |
| 1.350 | | | 0.277(0.093) |
| 1.492(+7) | | | 0.270(0.104) |

[a]Read as $1.068 \times 10^{1}$.

[b]Read as 1.39 ± 4.1%.

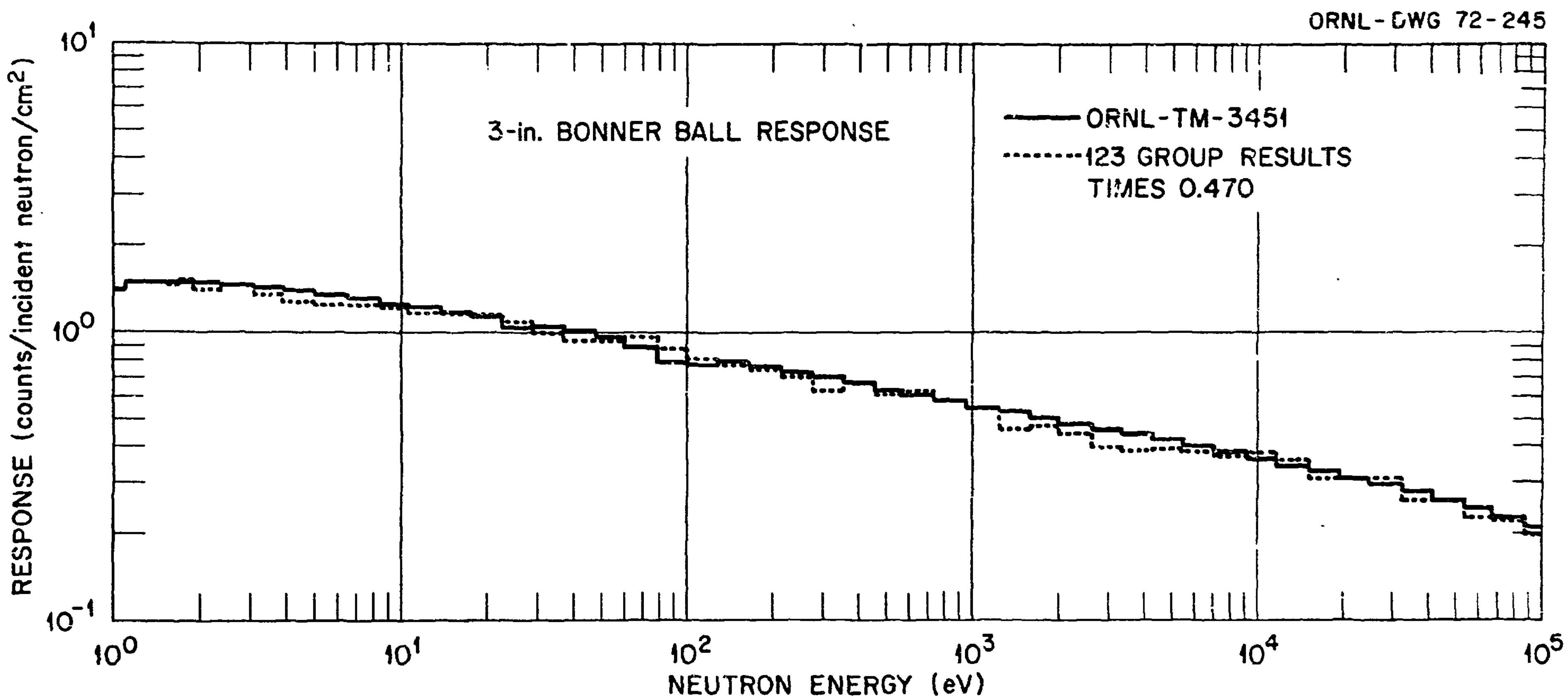


Fig. 2. Comparison Between ANISN and MORSE Calculated 3-in. Bonner Ball Response Functions.

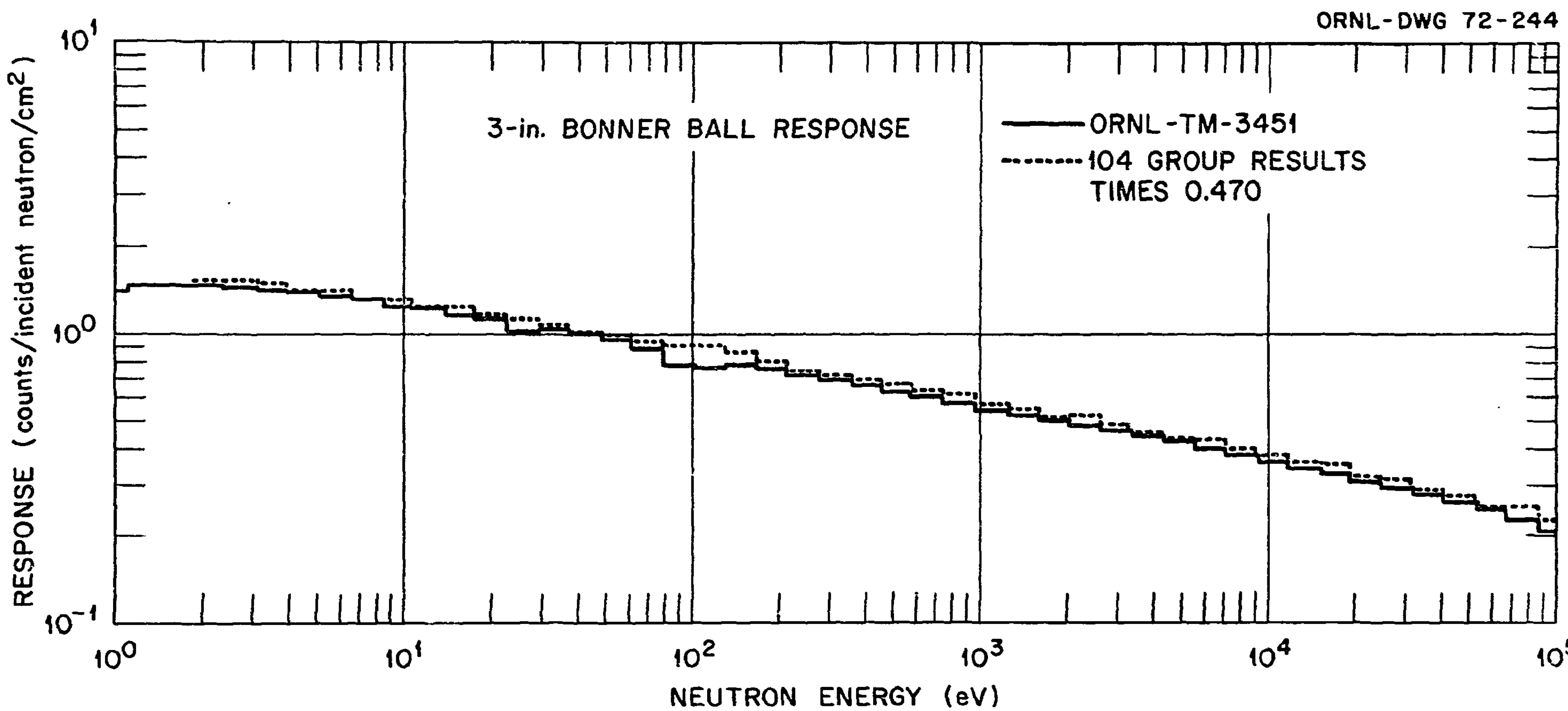


Fig. 3. Comparison Between ANISN and MORSE Calculated 3-in. Bonner Ball Response Functions.

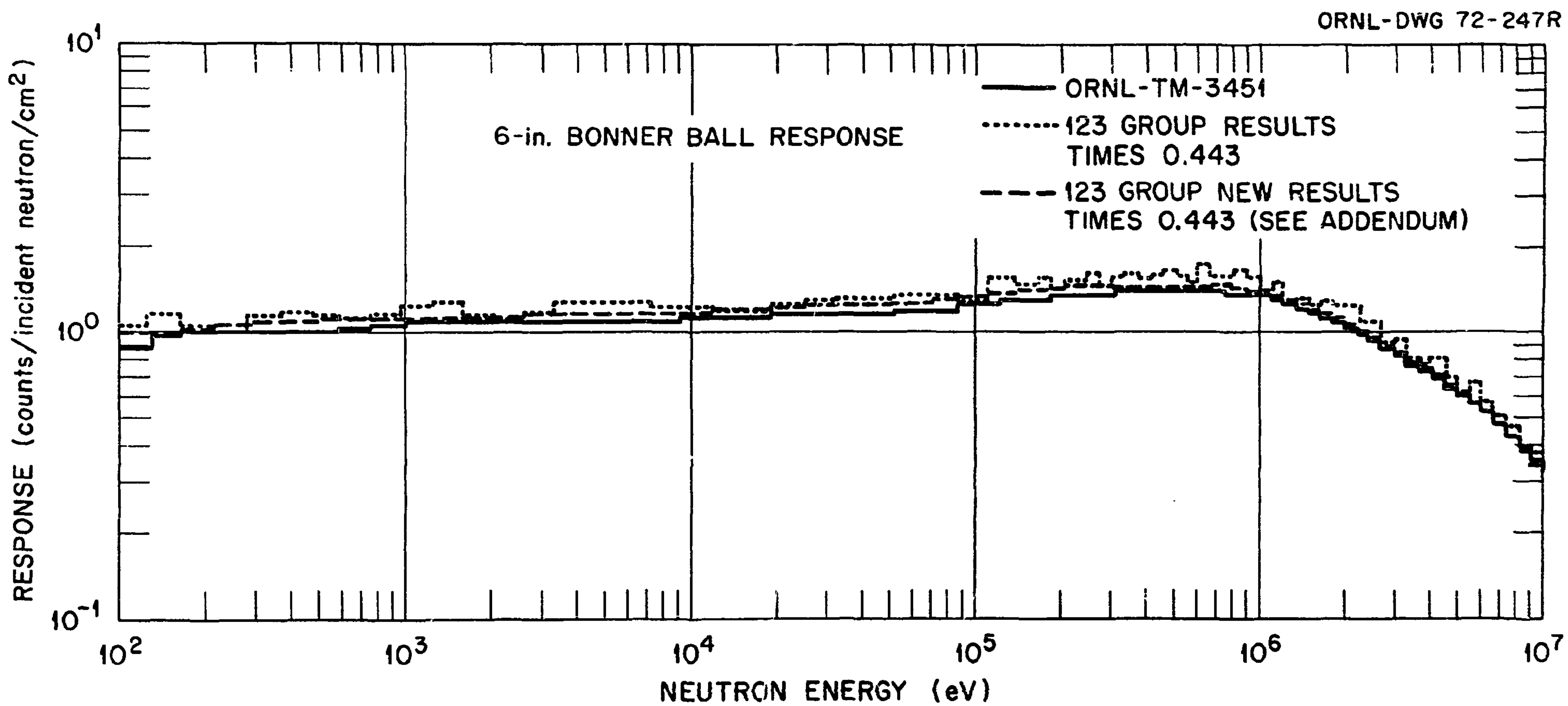


Fig. 4. Comparison Between ANISN and MORSE Calculated 6-in. Bonner Ball Response Functions.

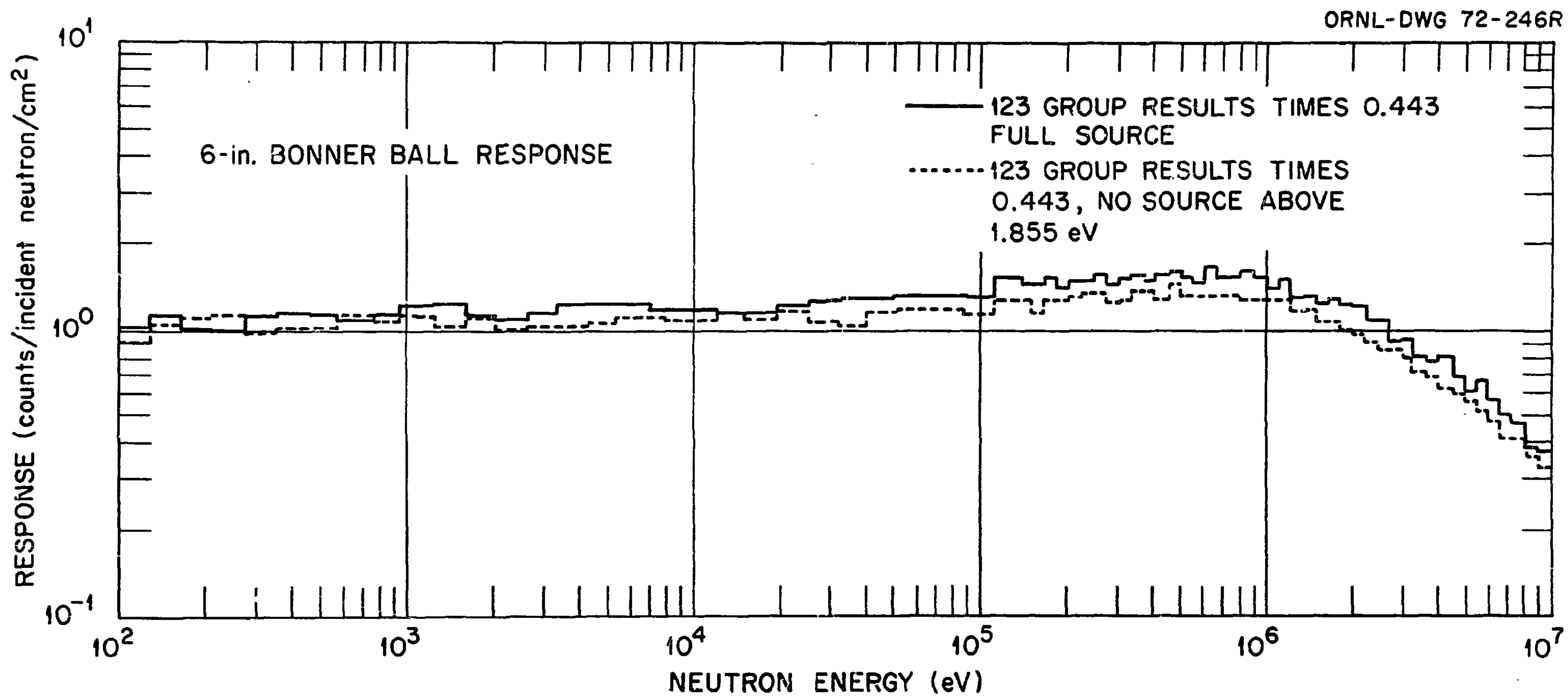


Fig. 5. Comparison of Calculated 6-in. Bonner Ball Response Functions With and Without Neutrons Above 1.855 eV.

1.855 eV. Thus, even the larger Bonner balls may be sensitive to the thermal neutron transport treatment.

The results described here utilizing MORSE with 123-group and 104-group cross sections were less than 10% different in magnitude from the ANISN calculations. The shape of the response functions was affected very little by the thermal neutron transport treatment. The method of calibration of the Bonner balls utilizes only the shape of the calculated response functions. The magnitudes are determined by folding known neutron spectra of calibrated sources with the calculated response functions. The ratio of measured counts to calculated counts for each Bonner ball is the "efficiency" of that detector. Although the differences in magnitude observed are not completely explained, they indicate no change in the previously determined response functions is required.

## Addendum

Additional ANISN calculations have been performed. These calculations utilized the identical 123-group cross sections and identical configuration and source as the MORSE calculations. The results for the 3-in. Bonner ball is essentially indistinguishable from the previous ANISN calculations which utilized single thermal group cross sections and a slightly different configuration. The new ANISN results for the 6-in. Bonner ball are within a few percent of the previous ANISN calculations above 1 MeV. Below 1 MeV, new results are 2-5% higher. The results for the 6-in. Bonner ball are shown in Fig. 4 as 123-group new results times 0.443.

REFERENCES

1. E. A. Straker, P. N. Stevens, D. C. Irving, and V. R. Cain, "The MORSE Code - A Multigroup Neutron and Gamma-Ray Monte Carlo Transport Code," ORNL-4585 (September 1970).

2. V. R. Cain, "SAMBO, A Collision Analysis Package for Monte Carlo Codes," ORNL CF 70-9-1 (1970).

3. E. A. Straker and M. B. Emmett, "MORSEC, A Revised Cross-Section Module for the MORSE Multigroup Monte Carlo Code," ORNL-4716 (1971).

4. N. M. Greene, J. L. Lucius, J. E. White, R. Q. Wright, C. W. Craven, Jr., and M. L. Tobias, "XLACS: A Program to Produce Weighted Multigroup Neutron Cross Sections From ENDF/B," ORNL-TM-3646 (to be published).

5. R. Q. Wright, J. L. Lucius, N. M. Greene, and C. W. Craven, Jr., "SUPERTOG: A Program to Generate Fine Group Constants and $P_n$ Scattering Matrices From ENDF/B," ORNL-TM-2679 (September 1969).

6. R. E. Maerker, L. R. Williams, F. R. Mynatt, and N. M. Greene, "Response Functions for Bonner Ball Neutron Detectors," ORNL-TM-3451 (June 1971).

7. R. E. Maerker, F. J. Muckenthaler, J. J. Manning, J. L. Hull, J. N. Money, K. M. Henry, and R. M. Freestone, Jr., "Calibration of the Bonner Ball Neutron Detectors Used at the Tower Shielding Facility," ORNL-TM-3465 (1971).